Dynamic Process Analysis and Hazard Prediction of Debris Flow in Eastern Qinghai-Tibet Plateau Area—A Case Study at Ridi Gully

Authors: Zou, Qiang, Zhou, Gordon G. D., Li, Shusong, Ouyang, Chaojun, and Tang, Jinbo

Source: Arctic, Antarctic, and Alpine Research, 49(3) : 373-390

Published By: Institute of Arctic and Alpine Research (INSTAAR), University of Colorado

URL: https://doi.org/10.1657/AAAR0017-019

Arctic, Antarctic, and Alpine Research, Vol. 49, No. 3, 2017, pp. 373–390
DOI: http://dx.doi.org/10.1657/AAAR0017-019

Dynamic process analysis and hazard prediction of debris flow in eastern Qinghai-Tibet Plateau area—A case study at Ridi Gully

Qiang Zou[1,2,*], Gordon G. D. Zhou[1,2], Shusong Li[3], Chaojun Ouyang[1,2], and Jinbo Tang[1,2]

[1]Key Laboratory of Mountain Hazards and Earth Surface Process/Institute of Mountain Hazards and Environment, Chinese Academy of Sciences (CAS), No. 9, Block 4, South Renmin Road, Chengdu, Sichuan, 610041, P.R. China
[2]University of Chinese Academy of Sciences, No.19(A) Yuquan Road, Shijingshan District, Beijing, 100049, P.R. China
[3]School of Environment and Resource, Southwest University of Science and Technology, 59 Qinglong Road, Mianyang, Sichuan, 621010, P.R. China
*Corresponding author's e-mail: zouqiangman@sina.com

A B S T R A C T

Process analysis and hazard prediction are essential for the prevention and mitigation of debris-flow hazards in mountainous areas. Many villages and ongoing infrastructure projects in China are vulnerable to large debris flows during heavy rainfall or glacier lake outbursts. Without emergency management planning, such contingencies can lead to extensive loss of life and egregious property damage. In the eastern Qinghai-Tibet Plateau area, debris-flow disasters are a common phenomenon. Taking Ridi Gully in the Sichuan Province of China as a case study, we analyzed the process of debris-flow events by running a dynamic erosion model. Because of the dynamic nature of the process, we needed to take into account many variables. Some of these variables include strong erosion in the origin area, scouring and downward erosion in debris-flow path, and siltation in accumulation area. Subsequently, we analyzed the elements underlying the hazard formation conditions and proposed a systematic and quantitative method of debris-flow hazard prediction based on kinetic energy and flow depth. Finally, we predicted the hazard and damage potential induced by the debris flow triggered by a 100-year and 200-year return period precipitation in Ridi Gully. The simulation results indicate that debris flow will cause great damage to the Sichuan-Tibet railway (or highway) and the residential area on the alluvial fan. This strongly suggests that, given the high level of debris-flow hazard predicted, the proposed method may serve as pertinent and timely support in planning measures to prevent or reduce the debris-flow hazard, both in the eastern Qinghai-Tibet Plateau area and beyond.

Introduction

The Qinghai-Tibet Plateau, with an average elevation of over 4000 m a.s.l., is often referred to as the roof of our Earth. Its mystic and beautiful landscape attracts a large number of visitors from both China and abroad. However, the geological environment and natural disasters in this area have also attracted worldwide attention. In this region of China, strong uplift of the Earth's crust creates a complex natural environment. This can present as active crustal stress, tremendous elevation differences, and dramatic climate change (Dhital, 2015). In the eastern area of the Qinghai-Tibet Plateau, large-scale natural disasters are a common occurrence. Specifically, conditions promoting debris flows are highly prevalent here. These conditions include things such as appropriate lithologic structures with loose materials and appropriate water resource conditions, which will be discussed later.

Debris flows can devastate local villages and infrastructure projects. Among these projects, the construction of the Sichuan-Tibet highway and the Sichuan-

Tibet railway are both critically affected by debris flows. These are the most significant transportation routes from Chengdu to Lhasa, the provincial capital cities in the provinces of Sichuan and Tibet, respectively. Thus, it is vital to develop a method to quantitatively analyze the dynamic process and associated hazards of debris flows in the eastern Qinghai-Tibet Plateau area.

Dynamic-process analysis and hazard assessment of debris flows play a crucial role in disaster prevention and mitigation. Although hazard assessment of debris flows is a challenge for disaster reduction in mountain regions worldwide (Okunishi and Suwa, 2001), scholars have recently made outstanding progress in regional studies and in on-site or local-scale studies (Jakob et al., 2005; Hürlimann et al., 2006; Fuchs et al., 2008; Calvo and Savi, 2009; Marzocchi, 2012; Zou et al., 2016). Generally, the regional assessment is based mainly on empirical and semi-quantitative analysis methods, such as GIS (Geographic Information System) spatial analysis (Huggel et al., 2003), statistical analysis (Mark and Ellen, 1995; Rickenmann, 1999), simple dynamic approaches (Archetti and Lamberti, 2003; Grêt-Regamey and Straub, 2006; Hübl et al., 2009), and interpretation of aerial photographs or satellite images (Bisson et al., 2005; Pradhan, 2010). In reference to risk assessment of individual debris-flow hazards and events that are focused on a local scale, scholars have explored various methods and models. For example, Anderson and Sitar (1996) proposed mechanisms of stress transfer to explain the initially drained deformation and established an appropriate stability analysis method. Gentile et al. (2008) applied a stability model that identifies areas with the potential for shallow landslides in different meteorological conditions. He proposed a risk analysis methodology to evaluate risk degrees of debris flows. He then implemented risk mapping in the torrential watersheds of the southern hillside of Gargano (Puglia, Italy). Sun et al. (2011) analyzed the dynamical processes of Donghekou rockslide debris flows triggered by the Wenchuan earthquake. These processes included five dynamic stages: the initiation stage, the acceleration of movement stage, the air-blast effect stage, the impact and redirection stage, and the long run-out slide-material accumulation stage. Ouyang et al. (2015) proposed a new method taking advantage of both the Coulomb and Voellmy frictional laws to simulate the stop-and-go process of debris flows. In this method, a new entrainment rate model coupled with the momentum conservation equation satisfying the boundary jump condition was proposed. Han et al. (2015) proposed a two-dimensional numerical model to simulate debris-flow behavior and the entrainment process. He also proposed a dynamic method to estimate the sediment entrainment rate. Additionally, some scholars analyzed the characteristics of debris flows that occurred after large earthquakes. They chose watersheds characterized by typical debris flows to discuss the implications with respect to risk (e.g., Cui et al., 2010, for the Wenchuan earthquake; and Lin et al., 2004, and Shou et al., 2011, for the Chi-Chi earthquake). These approaches for the evaluation of debris-flow risk vary significantly in terms of analysis and resulting numerical values. Furthermore, most of them are focused on a macroscopic view or qualitative description. Therefore, a method to quantitatively analyze the dynamic processes and hazards of on-site debris flows is necessary to develop appropriate risk management strategies for disaster prevention and mitigation.

This paper explores an analysis method for debris flow on a local scale. This is achieved by focusing on analyzing the dynamical processes and quantitative elements of hazard prediction of debris-flow events. Furthermore, the dynamic erosion model is applied to a case study of Ridi Gully, which is an area that has been significantly damaged by debris flows. Finally, we predict the hazard and damage potential induced by debris flows triggered by different return period precipitations in Ridi Gully.

Study Area

Location of the Study Area

Ridi Gully is located in Kangding County, Sichuan Province, China. It is situated on the right bank of the Wasi River, which is an anabranch of the upper reaches of the Dadu River (Fig. 1). In this area, between the Sichuan Basin and the Qinghai-Tibet Plateau, natural environmental conditions are complicated. One can find high mountains, torrential meanders, steep canyons, and diverse weather patterns here. It is an important location in terms of transport routes, as the G318 national road traverses the entrance of the gully and the Yaan-Kangding highway; soon, the Sichuan-Tibet railway will be built across it.

Formation Conditions of Debris Flows

Topographic Conditions

High mountains, deep-cut rivers, and steep slopes characterize the Ridi Gully. The gradient of slopes in the upper reaches (debris-flow source areas) of this valley reach 30°~70°. The main channel length is 10.48 km, and the catchment area is 25.87 km^2. The lowest point within the basin is located at the gully entrance at 1690 m a.s.l. The highest point is located in the southwest watershed at an elevation of 5917 m a.s.l. Using

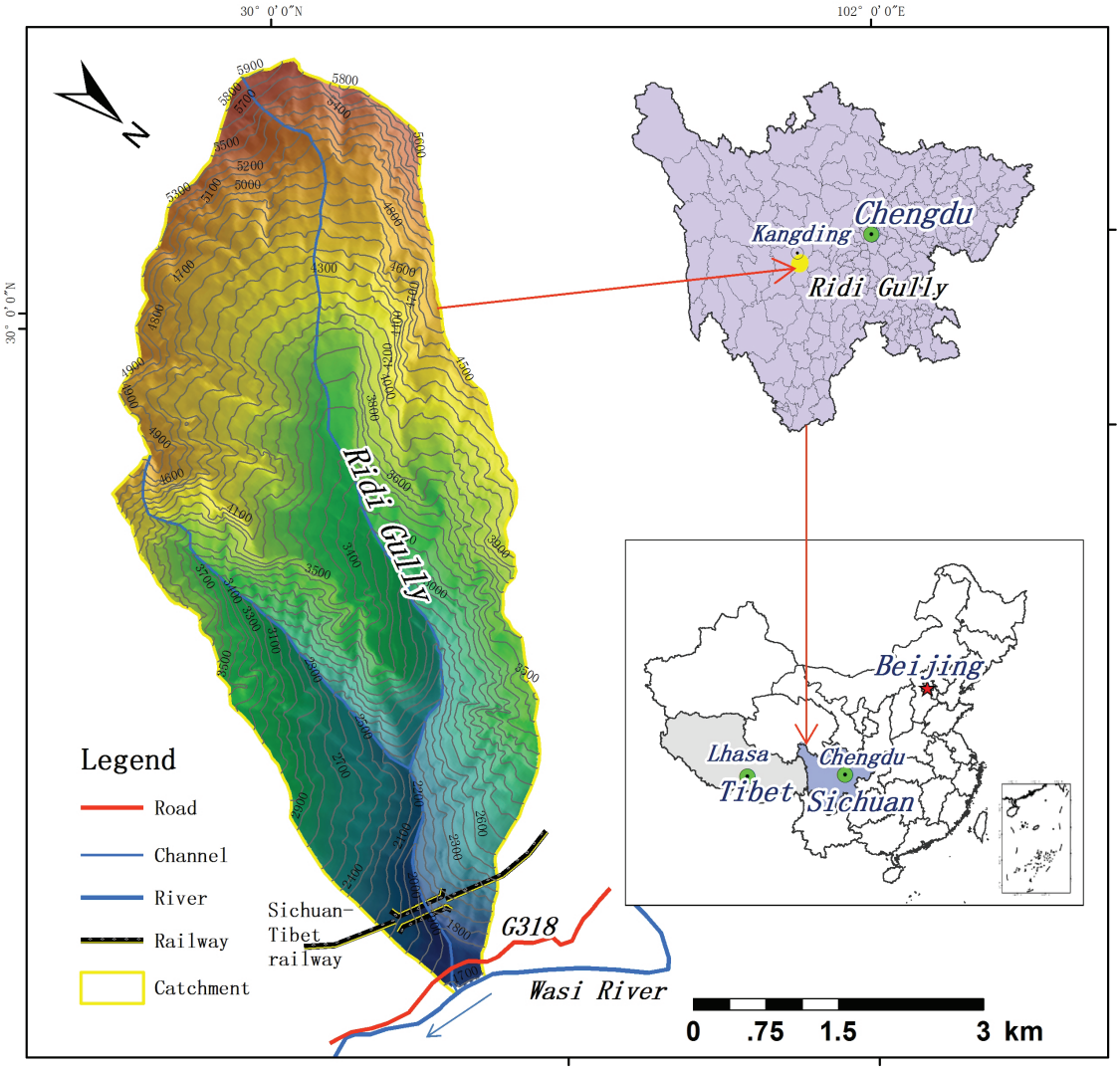

FIGURE 1. Location of the study area in eastern Qinghai-Tibet Plateau area, China.

data from field surveys and GIS technology, we obtained the following terrain parameters of the main and tributary channels: length of main channel, area of catchment, channel gradient, and relative elevation difference (Tables 1 and 2). The transverse section of gully channels presents a V-shape, and the longitudinal profiles typically range between 403 and 616‰. These terrain conditions are especially conducive to loose solid mass movement and debris-flow formation.

Geologic Conditions and Loose Solid Material

The geologic conditions of Ridi Gully are very complicated. The gully is located at the junction of the Longmenshan and Xianshuihe fault belts. Both of these faults are active geologic tectonic structures. The rock strata in this area are heavily fragmented by active tectonic activity. Fault and fracture development is extensive. As a result, rocks are especially susceptible to collapse from steep slope conditions (Fig. 2, part a). The exposed strata range mainly from the Sinian Period (Precambrian) to the Quaternary Period; rocks from the Cambrian Period are absent. The main lithology in this area includes plagiogranite, weathered granite, diorite, and metamorphic granite. A variety of loose accumulations from the Quaternary are distributed on the inclinations and riverbanks. Slide rocks, glacial deposits, and moraine deposits are distributed on the top of mountains and in gently sloping areas. Furthermore, pluvial alluvial sediments are located at the entrance of the gully, on the riverbed, and on river terraces. In addition, a large number of landslides and collapses occur on both sides of the main channel of the gully (Fig. 2, part b). Data from field investigation and remote sensors indicate that the detritus suffering from congelifraction by seasonal snow is a primary source for subsequent debris flow (Fig. 2, part c). According to the historical

TABLE 1

Topographical parameters of channels in Ridi Gully.

Channels	Area (km^2)	Length (km)	Slope of longitudinal profile (‰)	Elevation at entrance (m)	Elevation of highest point (m)	Largest relative elevation difference (m)
Main channel	25.87	10.48	403	1690	5917	4227
Tributary channel on left	17.14	8.01	462	2220	5917	3697
Tributary channel on right	4.83	4.50	616	2220	4991	2771

Table 2

Statistical results at each slope classification of Ridi Gully.

Channels	Items	Slope(°)				Summation
		<15	15~25	25~35	≥35	
Main channel	Area (km^2)	0.41	1.64	6.11	17.71	25.87
	Percentage(%)	1.58	6.34	23.62	68.46	100.00
Tributary channel on left	Area (km^2)	0.19	1.17	4.52	11.26	17.14
	Percentage(%)	1.11	6.83	26.37	65.69	100.00
Tributary channel on right	Area (km^2)	0.04	0.14	0.56	4.09	4.83
	Percentage(%)	0.83	2.90	11.59	84.68	100.00

FIGURE 2. Sources of loose solid materials for debris flow. (a) Slope failure, (b) bank collapse, and (c) moraine deposit.

records in the Kangding county annals, the study area has been repeatedly affected by IV–VII degree earthquakes. These earthquakes triggered a large number of landslides in the region and engendered abundant unconsolidated soil for debris flows. In short, the loose solid materials in Ridi Gully are readily available for debris-flow formation.

Water Resource Conditions

Ridi Gully is located in the eastern Qinghai-Tibet Plateau, which is a subtemperate zone with a subhumid climate. The characteristics of this climate include dry weather, abundant sunshine, great diurnal temperature differences, short summers, and long winter periods of ice and snow. According to the data from the local meteorological observation station, the annual average temperature is 7.1 °C, and the average temperature in January is –2.5 °C. Moreover, the maximum and minimum monthly average air temperatures are 15.7 °C and –14.7 °C, respectively, and the average annual precipitation is 803.8 mm. The precipitation from May to September accounts for 60 to 85% of the annual total (Fig. 3). During these months, storms and continuous rain are frequent. According to the local meteorological records, the maximum daily rainfall achieved is 65.9 mm, and the longest period of continuous rain lasted 58 days and accumulated to 542.9 mm of rainfall.

The study area is located on the right bank of Wasi River, which originates from Zheduo Mountain at an elevation of 4962 m a.s.l. The river has a large gradient and fierce water flow. It passes through the study area from northwest to southeast. Thus, this area is characterized by deep river incision, large relative elevation differences, and intensive periods of rainfall. This provides favorable water resource conditions for the formation of debris flows.

Methods

Dynamic Erosion Model for Debris Flows

Through analyzing the movement of debris flows in a natural environment, we found that the distance of movement in the direction of the debris flow is greater than its flow depth in the vertical direction. We can adopt mathematical integrals to describe fluid depth by using Navier-Stokes equations. Moreover, considering the gully bed erosion effect (Iverson, 2012), we deduced quality and momentum equations and boundary conditions, which are needed to satisfy the conditions between the debris-flow body and basement materials. A two-layer model, with an upper layer of moving flow and a bottom layer of erodible sediment beds, was defined as follows:

$$\frac{\partial(\bar{\rho}h)}{\partial t}+\frac{\partial(\bar{\rho}h\bar{u})}{\partial x}+\frac{\partial(\bar{\rho}h\bar{v})}{\partial y}-\bar{\rho}E=0 \tag{1}$$

$$\begin{aligned}&\frac{\partial(\bar{\rho}h\bar{u})}{\partial t}+\frac{\partial\left(\beta_{uv}\bar{\rho}h\bar{u}_1^2\right)}{\partial x}+\frac{\partial\left(\beta_{uv}\bar{\rho}h\bar{u}_1\bar{v}_1\right)}{\partial y}\\&-\bar{\rho}g_x h-k\rho g_z h\frac{\partial(h+z_b)}{\partial x}-\left(\tau_{1zx}\right)_b+\rho u_{1b}E\end{aligned} \tag{2}$$

$$\begin{aligned}&\frac{\partial(\bar{\rho}h\bar{u}_1)}{\partial t}+\frac{\partial\left(\beta_{uv}\bar{\rho}h\bar{u}_1\bar{v}_1\right)}{\partial x}+\frac{\partial\left(\beta_{vv}\bar{\rho}h\bar{v}_1^2\right)}{\partial y}\\&-k\rho g_z h\frac{\partial(h+z_b)}{\partial x}-\left(\tau_{1zx}\right)_b+\rho v_{1b}E\end{aligned} \tag{3}$$

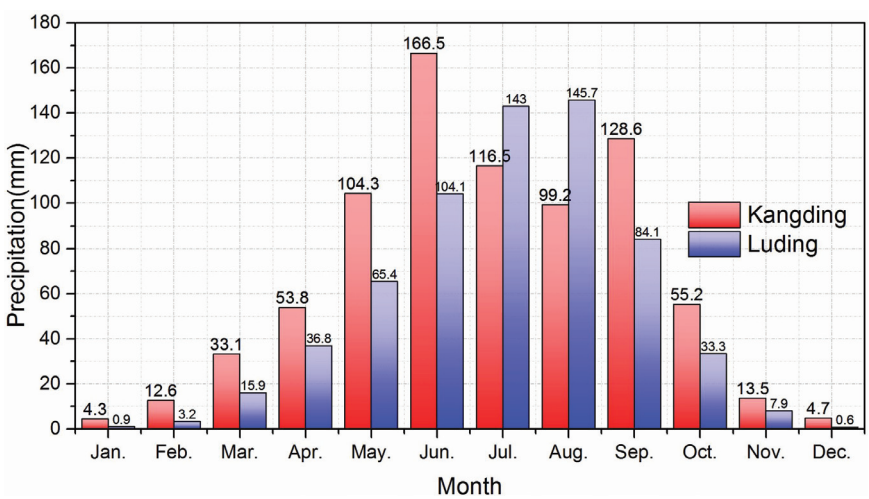

FIGURE 3. The average monthly precipitation at Kangding and Luding meteorological stations in the study area.

$$E = -\frac{\partial z_b}{\partial t} = \alpha h v, \tag{4}$$

where $\bar{\rho}_1$ is the average fluid density (kg/m^3); h is flow depth (m); $\bar{u}_1$ is the velocity in the x direction (m/s); $\bar{v}_1$ is the velocity on the y direction (m/s); E is erosion rate; β_{uu}, β_{uv} ,β_{vv} are momentum distribution coefficients on different directions; g_x , g_y , g_z are three components of gravitational acceleration on the x, y, z coordinate directions (m/s^3); K is the coefficient of earth pressure, Z_b is the terrain height of gully bed (m); $(\tau_{1zx})_b$,$(\tau_{1zy})_b$ are the basal resistance on the x and y coordinate directions, respectively; v_{1b} is basal fluid velocity (m/s); V is average velocity of fluid (m/s); and α is the coefficient of erosion rate, which can be calculated by the following formula (Ouyang et al, 2015):

$$\alpha = \frac{1n\left(V_f / V_0\right)}{\bar{S}}, \tag{5}$$

where, V_f is the final accumulation volume of debris flow (m^3), V_0 is the initial volume of debris flow (m^3), V_f/V_0 represents the amplification coefficient of the magnitude of debris flow, and $\bar{S}$ is average moving distance of debris flow (m). These parameters can be obtained through field investigation or analysis of historical disaster data. The Coulomb-Voellmy coupling model is adopted to calculate basement resistance for a viscous debris flow. There are two methods for calculating the basement resistance. If debris-flow velocity is high, the basement resistance can be determined by:

$$\tau = \mu g h + g\frac{U^2}{h\xi}, \tag{6}$$

If flow velocity is small or debris flow tends to be static, the following formula is used to calculate basement resistance:

$$\tau = gh \tan(\delta), \tag{7}$$

where τ is the basement resistance, μ is the friction coefficient, ξ is the turbulent coefficient, h is flow depth (m), U is the average velocity of debris flow (m/s), and δ is the frictional angle (°).

Method of Debris-Flow Hazard Prediction

Three extremely significant civil engineering projects traverse Ridi Gully: the G318 national road, the Yaan-Kangding highway, and the Sichuan-Tibet railway. According to our investigations, debris flows in Ridi Gully will bring serious hazards to such engineering projects. These mainly include (1) depositing the clearance of the bridge, (2) impacting the foundation or pier of the bridge, and (3) burring or scouring the highway.

In order to analyze the hazard characteristics of debris flows occurring in Ridi Gully, we propose a systematic and quantitative hazard analysis method supported by numerical simulation of debris-flow movement. The proposed model is expressed as:

$$H = H_e + H_d, \tag{8}$$

where H is the total hazard degree, H_e is the hazard caused by the impact force of the debris flow indexed to the maximum kinetic energy value in each grid during the whole debris-flow movement process, and H_d is the hazard caused by debris-flow silting indexed to flow depth.

Methods for Determining the Silting Depth of Debris Flow

Flow velocity is a key parameter for identifying the impact force of debris flows, while flow depth can reflect the silting hazard. In this article, we simulate the debris-flow movement process in an alluvial area by adopting the numerical approach detailed in the section Dynamic Erosion Model for Debris Flow. Using a Digital Elevation Model (DEM) of the study area, we identify the spatial distributions of velocity and flow depth for each grid square during the movement process. To determine silting damage, the maximum flow depth of the debris flow is adopted. The flow depth of each grid (i,j) can be calculated using the following formula:

$$H_d = \max(h) = \frac{Nn_{i,j}\Delta V}{A}, \tag{9}$$

where $Nn_{i,j}$ is the number of particles on grid (i,j) at time n, ΔV is the average volume of each particle (m^3), A is the grid area (m^2), h is the flow depth (m), and H_d is the silting degree or maximum deposit depth (m). Generally, larger values of H_d represent a more serious hazard.

Methods for Determining the Impact Force of Debris Flows

To quantitatively characterize the largest impact hazard at each grid position, we index the impact force

and damage capability of a debris flow by applying the maximum kinetic energy. This process allows us to calculate the impact degree of each grid square for the entire dynamic debris-flow process. The simulation starts from the gully mouth (at the top of the alluvial fan) and is implemented by determining

$$H_e = A.\max_{t>0}\left[\left(u^2+v^2\right)h\rho\right]$$
$$u = \frac{1}{nn_{ij}}\sum_{k=1}^{Nn_{ij}} u_k \quad , \qquad (10)$$
$$V = \frac{1}{Nn_{ij}}\sum_{k=1}^{Nn_{ij}} V_k$$

where H_e is the maximum value of the kinetic energy of the debris flow ($N{\cdot}m$), u and v are the velocities (m/s) in the x and y directions, respectively, h is the flow depth (m), ρ is the density of the debris flow (t/m^3), and A is the grid area (m^2). $Nn_{i,j}$ is the number of particles on the grid (i,j) at time n, and u_k, v_k are the velocities (m/s) for the k-th particle on grid (i,j), respectively.

Data Normalization Method

Because the dimensions of H_e and H_d index are different, we need to normalize these hazard parameters. We normalize the indexes by adopting the following approach:

$$H_i' = \frac{H_i}{H_{\max}}, \qquad (11)$$

where H_i' indicates the normalized value of the hazard degree, and H_i is the initial hazard index, $H_{\max}$ is the maximum hazard index H_e or H_d in the study area.

Application and Results

Erosion Process of Debris Flow

According to the variations in vertical elevation, valley landform, and unconsolidated soil distribution in Ridi Gully, we divide the gully into three different partitions: the origin area, the transition area, and the accumulation area (Fig. 4).

Erosion in the Debris-Flow Origin Area

The debris-flow formation area is located above 3550 m a.s.l. in the upstream area of Ridi Gully. The main channel has a V-shape, and its average gradient is 540‰. Both sides of the main channel are steep inclinations with the slope ranging from 30° to 50°. Data from remote sensors indicate the main channel is seasonally covered by snow. A glacier, with an area of 1.95 km^2, is located at 4520 m a.s.l. Because of the large gully gradient and strong frost weathering, the detritus, suffering from congelifraction, is vulnerable to being triggered by these hydrodynamic conditions into inducing a severely hazardous debris flow. Therefore, strong erosion is the main feature in this debris-flow origin area.

Erosion in the Debris-Flow Transition Area

The transition area is located in the middle and downstream reaches of Ridi Gully, at an elevation between 1780 m a.s.l. and 3500 m a.s.l. Here the longitudinal gradient of the main channel is 319‰. This section represents the main transport channels of debris flows. There is vegetation on both sides of the main channel. The valley slopes vary from 40° to 55°. According to field investigation and interpreted data from remote sensors, the slumped mass on both sides of the channel is unstable. With the effects of intensive rainfall and flash

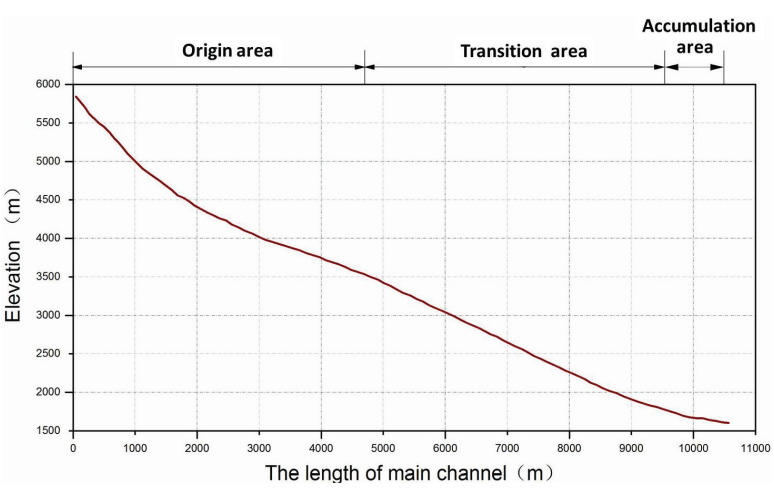

FIGURE 4. The longitudinal profile of main channel of Ridi Gully.

flooding, this loose solid material would enter into the channel and amplify the magnitude of debris flow. Thus, scouring and downward erosion are two main erosion processes in the debris-flow transition area.

Erosion in Debris-Flow Accumulation Area

The accumulation area, which lies at an elevation between 1690 m a.s.l. and 1780 m a.s.l., is fan-shaped and characterized by flat and open terrain. The channel length is 0.60 km, the average longitudinal gradient is 150‰, with a gentle slope between 6° and 12°. The average width of this area is 130 m to 650 m. From image analysis and field investigation, it was determined that the degree of vegetation coverage on both sides of the channel is high and that the gradient of the channel is relatively small. These conditions are conducive to the accumulation of debris-flow deposition. In addition, there is a thick stack of stratum from debris flows in this deposition area, the magnitude of which is approximately 2.3×10^6 m^3. Under the effects of the terrain, the flow velocity and transporting capacity of a debris flow deceases upon entering this area. The debris is deposited in the alluvial fans. Therefore, siltation and burying are the main characteristics of the debris-flow accumulation area.

Parameters Input for the Simulation

Debris-Flow Density

Through field surveys and visits by locals, we obtained the basic parameters of the debris flow: length of main channel, area of catchment, channel slope, and particle size. To determine the characteristics and properties of the source materials of a debris flow, we took samples of actual source materials of debris flows in Ridi Gully and then performed a direct shear test and analyzed particle properties (Fig. 5). The Malvern test of grain-size distribution showed two peaks in the fine particle fraction (below 2 mm) with peak points at 0.01 mm and 0.4 mm in sample #1, and 0.02 mm and 0.04 mm in sample #2 (Figs. 6 and 7). These results illustrate that the structure of the debris material undergoes a certain change during the movement process from hillside to channel. The particles in the formation area start to move, and then form a debris flow, and then under the effect of slowing terrain, these particles stop in the deposition area. This process is consistent with what was determined from field observations.

These results and the measured grain-size distribution were then used to calculate the density of debris-flow material in Ridi Gully using Equation (12) (Chen et al., 2003). The calculated value was 2.1 g/cm^3, which showed that the debris flow in Ridi Gully is viscous under the classification standard of debris flows in China.

$$\gamma = -1.32 \times 10^3 x^7 - 5.13 \times 10^2 x^6 + 8.91 x^5 - 55 x^4 + 34.6 x^3 - 67 x^2 + 12.5 x + 1.55, \quad (12)$$

where x is the percentage of clay content in the resulting deposit.

Dynamic Parameters of Debris Flows

For the following discussion on hazard prediction, some dynamic parameters, including the flood peak discharge (Q_B), the debris-flow peak discharge (Q_C), the debris-flow velocity (V_C), and the total volume of one debris flow (Q_t) need to be determined.

Flood Peak Discharge

The flood peak discharge (Q_B) of Ridi Gully should be determined for the following calculation of debris-

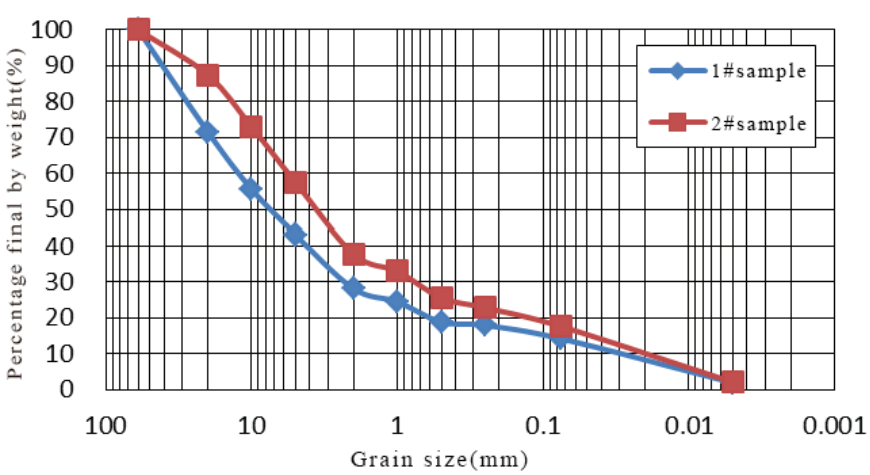

FIGURE 5. The grain-size distribution of the debris flow deposits in Ridi Gully.

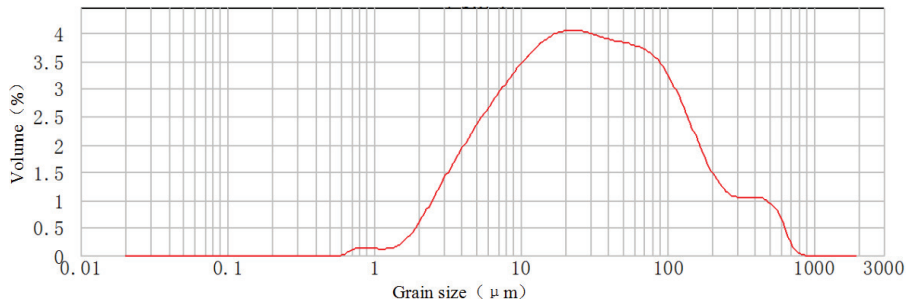

FIGURE 6. Malvern curve of sample #1 in Ridi Gully.

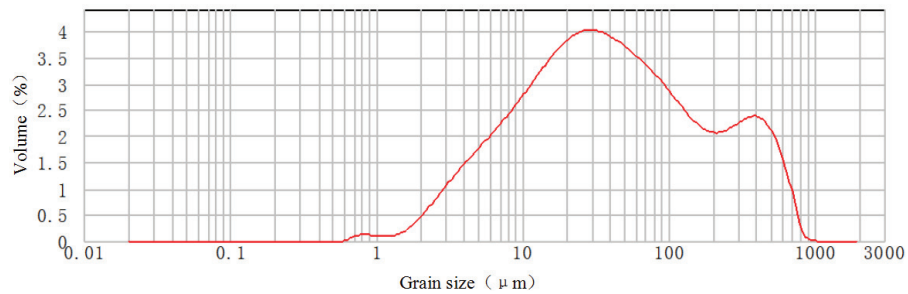

FIGURE 7. Malvern curve of sample #2 in Ridi Gully.

flow peak discharge (Q_C). The flood peak discharge (Q_B) can be calculated from Zhou et al. (1991):

$$Q_B = 0.278\varphi \frac{S}{T^n} F, \tag{13}$$

where F is the watershed area (m^2), φ is the runoff coefficient of flood peak, S is the rainfall intensity (mm), T is the runoff confluence time of the rainfall(s), and n is the attenuation index of the rainfall. The parameter F can be directly calculated and measured from the topographic map by using GIS technology. S, T, φ, and n can be determined by the following empirical equations (Liu et al., 2012):

$$S = \bar{H}_1 K_1, \tag{14}$$

$$T = \left[\frac{0.383}{mS^{1/4}/\theta}\right]^{\frac{4}{4-n}}, \tag{15}$$

$$\varphi = 1 - \frac{\mu}{S} T^n, \tag{16}$$

$$n = 1 + 1.285\left(1g\frac{\overline{H_1}K_1}{H_6K_6}\right), \tag{17}$$

$$m = 0.318\theta^{0.204}, \tag{18}$$

$$\theta = \frac{L}{J^{1/3}F^{1/4}}, \tag{19}$$

$$\mu = 3.6K_P F^{-0.19}, \tag{20}$$

where K_1 and K_6 are the modulus coefficients for the variation coefficient CV_1 and CV_6, respectively; m is the runoff confluence parameter; θ is the catchment characteristic parameter; L is the channel length (m); J is the longitudinal slope of the channel; μ is the runoff yield parameter; and KP is the modulus coefficient under different return periods.

To calculate the parameters above, some rainfall data, including the 1-hour (H_1) and 6-hour (H_6) average rainfall intensities and the corresponding coefficients of variation (CV_1 and CV_6) can be obtained from the rainfall contour maps from *The Rainstorm and Flood Calculation Manual of Medium and Small Basins in Sichuan Province* (Sichuan Provincial Water Conservancy and Electric Power Department, 2010; rainfall data from 1978 to 2004). Then based on the basic parameters and calculations from the formulas above, we can obtain the flood peak discharge with different flood frequencies in the main channel and tributary channels of Ridi Gully. The results are listed in Table 3.

Debris-Flow Peak Discharge

The debris-flow peak discharge (Q_c) can be calculated by using Equation (21) (Fei and Shu, 2004):

TABLE 3

Basic parameters and flood peak discharge of Ridi Gully.

Channels	P (%)	Area of catchment (km^2)	Length of main channel (km)	Average channel slope (‰)	$\overline{H_1}$ (mm)	C_{V1}	K_{P1}	H_{1P} (mm)	$\overline{H_6}$ (mm)	C_{V6}	K_{P6}	H_{6P} (mm)	$\overline{H_{24}}$ (mm)	C_{V24}	K_{P24}	H_{24P} (mm)	θ	m	μ	τ	S_P (mm)	Q_B (m^3/s)
Main channel	0.5	25.87	10.48	403	14.00	0.50	3.06	42.84	25.00	0.35	2.29	57.25	40.00	0.30	2.06	82.40	6.29	0.32	3.42	4.31	42.84	83.34
	1						2.74	38.36			2.11	52.75			1.92	76.80			3.22	4.46	38.36	72.35
	2						2.42	33.88			1.92	48.00			1.77	70.80			3.03	4.64	33.88	61.43
	5						1.99	27.86			1.67	41.75			1.57	62.80			2.76	4.92	27.86	47.86
Tributary channel on left	0.5	17.14	8.01	463	14.00	0.50	3.06	42.84	25.00	0.35	2.29	57.25	40.00	0.30	2.06	82.40	5.09	0.31	3.69	3.44	42.84	54.51
	1						2.74	38.36			2.11	52.75			1.92	76.80			3.48	3.56	38.36	47.44
	2						2.42	33.88			1.92	48.00			1.77	70.80			3.27	3.71	33.88	40.37
	5						1.99	27.86			1.67	41.75			1.57	62.80			2.98	3.94	27.86	31.61
Tributary channel on right	0.5	4.83	4.50	618	14.00	0.50	3.06	42.80	25.00	0.35	2.29	57.25	40.00	0.30	2.06	82.40	3.56	0.29	4.70	2.39	42.84	21.25
	1						2.74	38.36			2.11	52.75			1.92	76.80			4.43	2.48	38.36	18.34
	2						2.42	33.88			1.92	48.00			1.77	70.80			4.16	2.59	33.88	15.47
	5						1.99	27.86			1.67	41.75			1.57	62.80			3.79	2.76	27.86	11.90

$$Q_C = (1+\phi)Q_B D_U$$
$$\phi = (\gamma_c - \gamma_W)/(\gamma_s - \gamma_c) \quad (21)$$

where Q_c is the peak discharge of debris flow (m^3/s); Q_B is the peak discharge of flood (m^3/s); D_U is the blockage coefficient, which shows the quantity of landslide deposits in the channels; ϕ is the increase coefficient of debris-flow peak discharge; γ_c is the density of debris flow (t/m^3); γ_W is the water density (t/m^3), which is usually determined as 1.00 t/m^3; and γ_s is solid matter density (t/m^3), which is usually given as 2.7 t/m^3.

Usually, the blockage degree is classified as very serious blockage (D_U = 3.0–2.5), serious blockage (D_U = 2.5–2.0), normal blockage (D_U = 2.0–1.5), or minor blockage (D_U = 1.5–1.0) (Wu et al., 1993). Based on the field investigations and inspection of aerial photographs, the blockage coefficient of Ridi Gully is considered to be 2.5–2.0 (serious blockage). The debris-flow peak discharge (with different flood frequencies in the main channel and tributary channels) of Ridi Gully are listed in Table 4.

Debris-Flow Velocity

The debris-flow velocity (Vc) can be calculated by using Equation (22) (Zhou et al., 1991; Fei and Shu, 2004):

$$V_C = \frac{1}{n_C} H_C^{2/3} I_C^{1/2} \quad (22)$$

where, H_C is the hydraulic radius of the debris flow, I_C is the hydraulic slope, and n_C is the roughness coefficient. The debris-flow velocity with different flood frequencies in the main channel and tributary channel of Ridi Gully is list in Table 5.

Debris-Flow Volume

The total volume of one debris flow (Q_t) can be calculated by using Equation (23) (Cui et al., 2013). Subsequently, the total amount of solid material of one debris flow (W_c) can be obtained using Equation (24) (Chen, 2011):

$$Q_t = 152.97 Q_c^{1.266} \quad (23)$$

$$W_C = (\gamma_C - \gamma_w).Q_t / (\gamma_S - \gamma_w) \quad (24)$$

where, Q_t is total runoff of a single debris flow (m^3), Q_c is the peak discharge of a single debris flow (m^3/s), and W_c is the total amount of solid material in a single debris flow (m^3).

Using the formulas above, the total volume of one debris flow and the total amount of solid material in Ridi Gully can be calculated (Table 6).

Dynamic-Process Simulation of Debris Flows

The input parameters required for simulation were obtained through calculation. Then, the debris-flow mo-

TABLE 4

Debris flow peak discharge of Ridi Gully.

Channels	P (%)	γ_c (t/m^3)	D_U	Q_C (m^3/s)
Main channel	0.5	2.20	3.00	916.73
	1	2.10	2.80	607.77
	2	2.00	2.60	405.45
	5	1.90	2.40	252.70
Tributary channel on left	0.5	2.20	3.00	599.60
	1	2.10	2.80	398.46
	2	2.00	2.60	266.46
	5	1.90	2.40	166.90
Tributary channel on right	0.5	2.20	2.80	218.20
	1	2.10	2.60	143.05
	2	2.00	2.40	94.27
	5	1.90	2.20	57.59

TABLE 5

Debris flow velocity of Ridi Gully.

Channels	P (%)	I	V_C (m/s)
Main channel	0.5	0.163	7.03
	1	0.163	6.29
	2	0.163	5.50
	5	0.163	4.65
Tributary channel on left	0.5	0.312	8.70
	1	0.312	7.61
	2	0.312	6.44
	5	0.312	5.14
Tributary channel on right	0.5	0.236	7.57
	1	0.236	6.62
	2	0.236	5.60
	5	0.236	4.47

TABLE 6

The total volume of one debris flow and the total amount of solid material in Ridi Gully.

Channels	P (%)	Q_t (10^4 m^3)	W_c (10^4 m^3)
Main channel	0.5	174.18	126.68
	1	86.61	57.74
	2	38.52	23.34
	5	16.00	8.73
Tributary channel on left	0.5	104.43	75.95
	1	50.47	33.65
	2	21.09	12.78
	5	7.93	4.32
Tributary channel on right	0.5	20.73	15.08
	1	9.06	6.04
	2	4.48	2.71
	5	1.82	0.99

tion process on the alluvial area were simulated with the support of DEM data in a 5 m × 5 m grid. By analyzing this dynamic process of debris flow in Ridi Gully, we determined that the initial debris-flow source material triggered by a 100-year return period precipitation was 86.61×10^4 m^3, whereas 174.18×10^4 m^3 was triggered by a 200-year return period precipitation. The simulation results (Figs. 8 and 9) show that a debris flow moves rapidly in the upstream area, while with the decreasing gradient and narrowing of gully channels, debris starts to deposit and the flow depth begins to increase. In addition, the velocity of a debris flow triggered by a 200-year return period precipitation is larger than that triggered by a 100-year return period precipitation. Furthermore, during the dynamic process of debris flow in Ridi Gully, the flow depth achieved the maximum value at the location of the railway bridge, about 1200 s after initiation for the 100-year return period precipitation, and after only 900 s for the 200-year return period precipitation.

Hazard Prediction of Debris Flow

According to the simulation results, we can evaluate the potential hazard induced by debris flow in Ridi

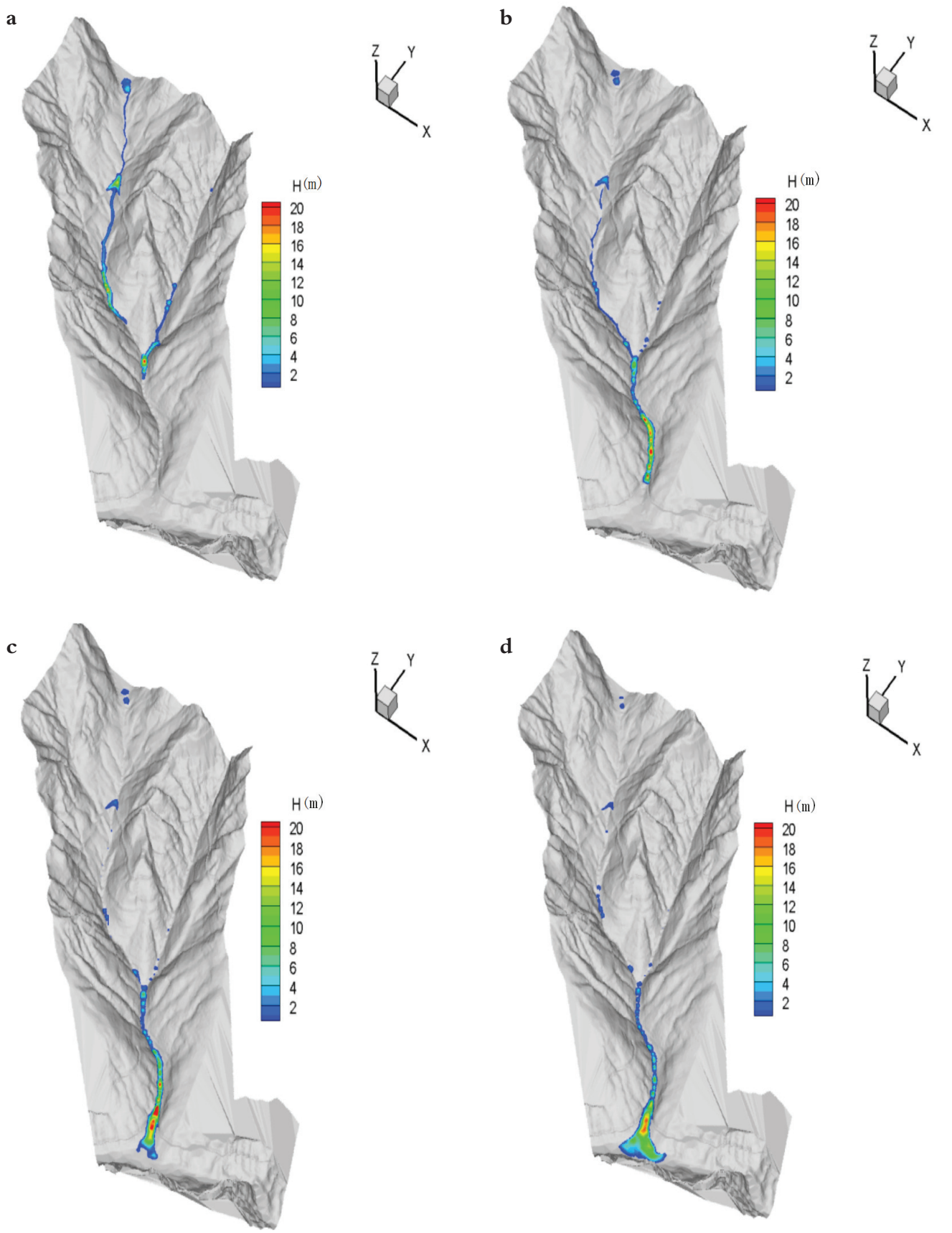

FIGURE 8. The snapshots of flow depth in Ridi Gully following a 100-year return period precipitation. (a) t = 150 s, (b) t = 600 s, (c) t = 900 s, and (d) t = 1500 s.

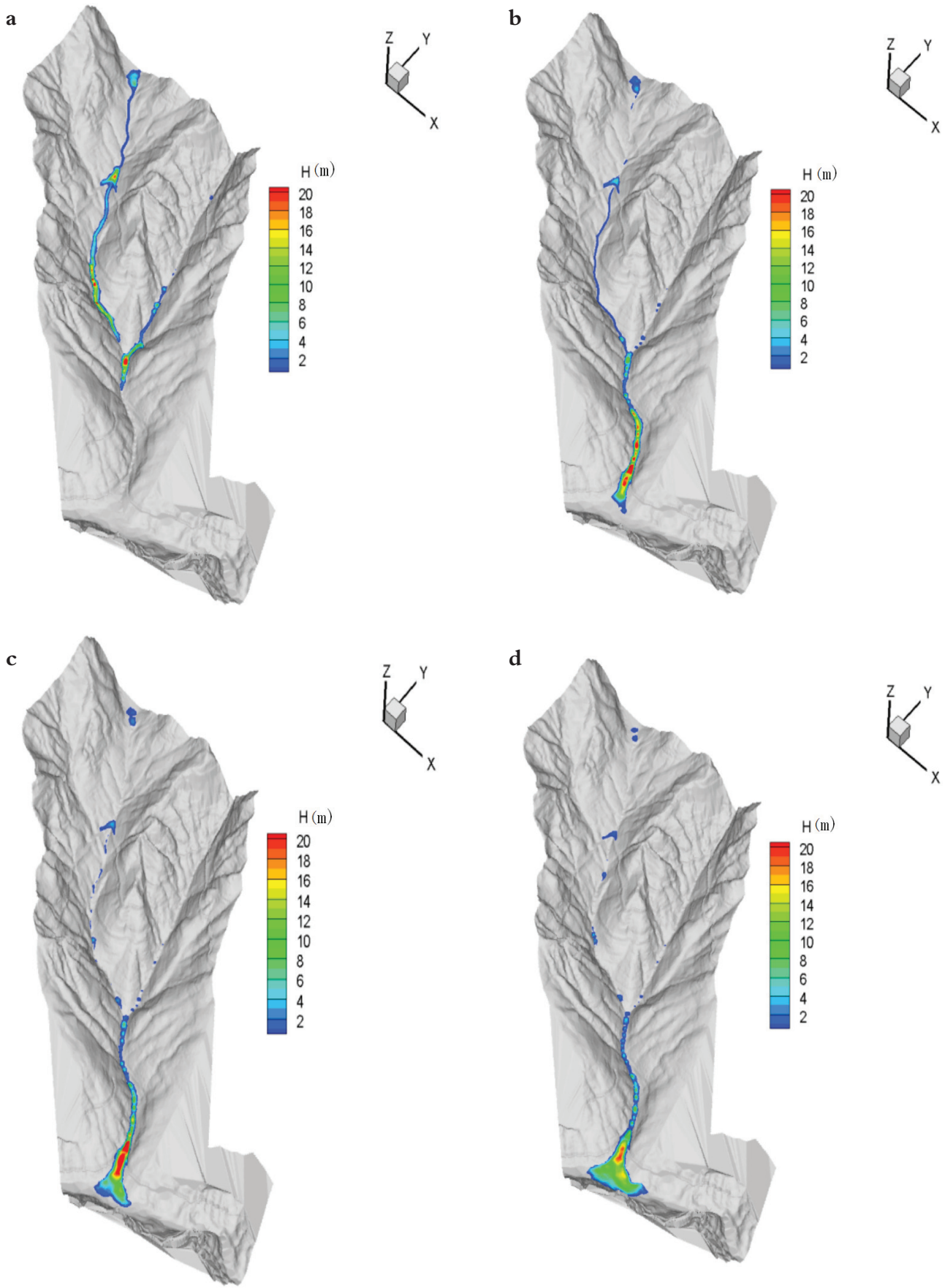

FIGURE 9. The snapshots of flow depth in Ridi Gully following a 200-year return period precipitation. (a) t = 150 s, (b) t = 600 s, (c) t = 900 s, and (d) t = 1500 s.

Gully. Considering the highest risk of debris flow to the hazard-affected objects, we used the maximum simulated value during the dynamic process to estimate the hazard of debris flow in Ridi Gully. By applying GIS spatial analysis techniques, we extracted the channel profile sections of Ridi Gully. Specifically, at the location of the channel bridge section crossed by the Sichuan Tibet Railway, the depth of the debris flow was 8.5 m following a 100-year rainfall and 13.8 m following a 200-year rainfall. Subsequently, we compared the simulated results with the 18 m headroom design of the Sichuan-Tibet Railway (Fig. 10). It shows that half of the height of the designed headroom will be occupied by the debris flow following a 100-year return period precipitation, and nearly two-thirds of the height of designed headroom will be occupied by debris flow following a 200-year return period precipitation (Fig. 11). With the effect of steep terrain, the scouring erosion of the debris flow on the Sichuan-Tibet Railway is enhanced. The G318 national road and villages in the alluvial area of the Ridi Gully also have a potential for high risk from debris-flow hazards. Considering the composite effects of impacting hazards, burying hazards, and scouring erosion, the hazards of debris flow are high to very high in the Ridi Gully. Therefore, to reduce the damage induced by debris flows, scientific engineering measures are required to control debris flows and to establish a real-time warning system to predict debris flows.

Discussion

Based on the dynamic erosion model and numerical simulation for debris flow, we analyzed the erosion and hazard characteristics involved in the dynamic process of debris flow in Ridi Gully. In this analysis, some empirical equations (such as Equations [12] and [21]) were applied to calculate debris-flow dynamic parameters. Although these equations were often used in previous studies (You et al., 2010; Liu et al., 2012; Xiang et al., 2012; Cui et al., 2013), more accurate tests are necessary to further improve the precision of these empirical equations as well as to develop better theoretical models. For instance, the debris-flow density calculation (Equation [12]) was established based on over 100 tests and in-

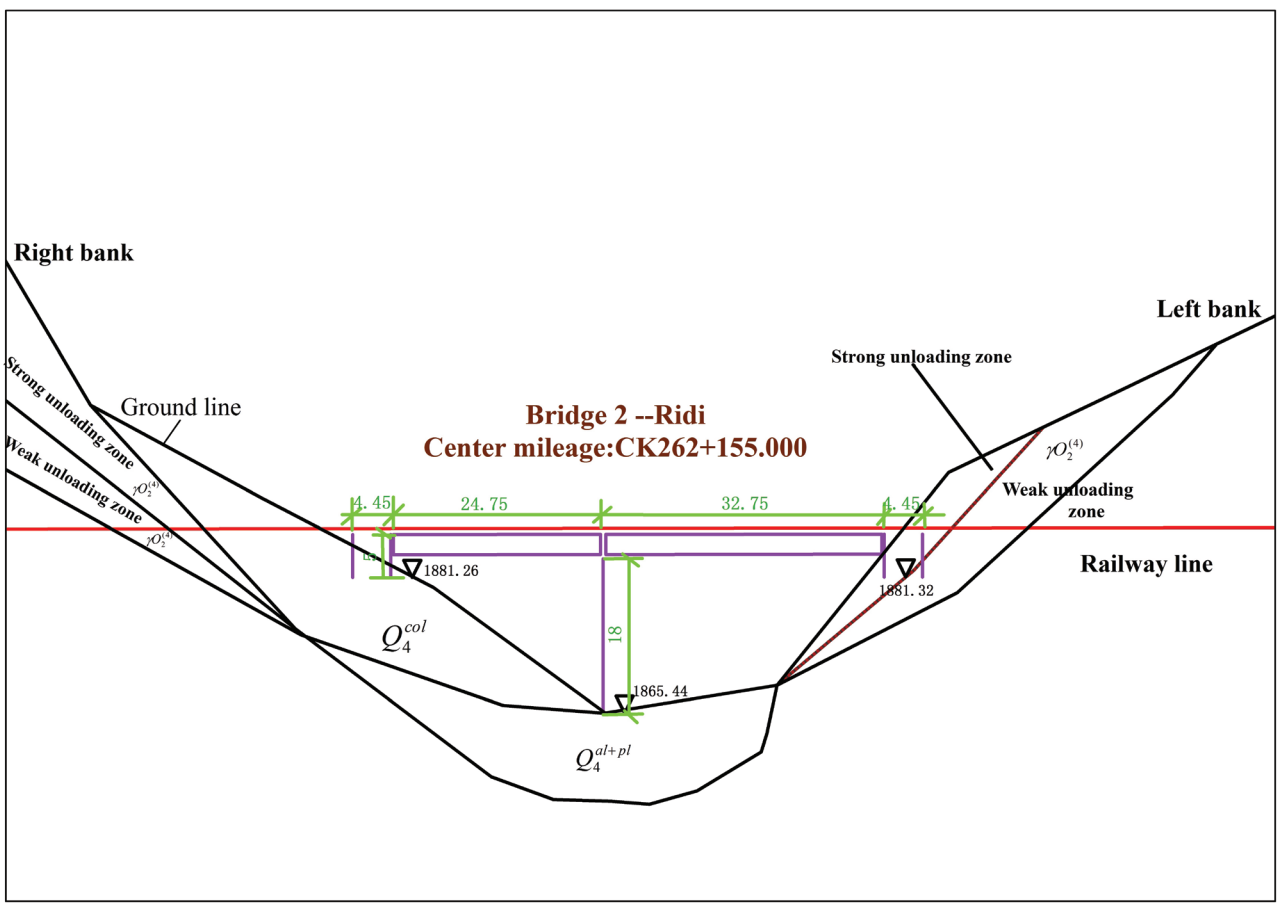

FIGURE 10. The section profile of Sichuan-Tibet Railway across Ridi Gully.

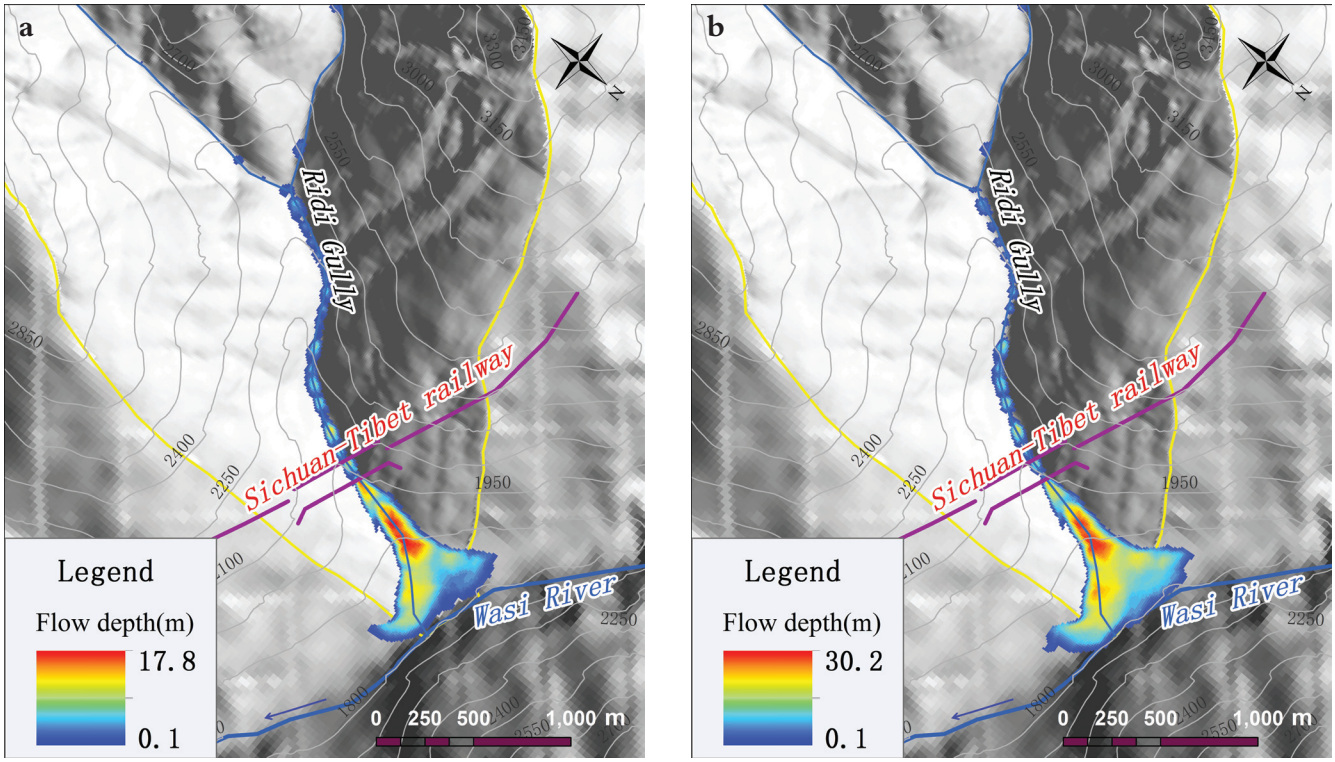

FIGURE 11. Simulated results of the Sichuan-Tibet Railway section in Ridi Gully. (a) Simulated result following a 100-year return period precipitation. (b) Simulated result following a 200-year return period precipitation.

vestigated data sets; however, there exists an opportunity for improvement by replacing the current polynomial equation with a theoretical model based on dimensional analysis. In addition, the eastern Qinghai-Tibet Plateau areas are affected by earthquakes. Although the blockage degree D_U was adopted to illustrate the surface disturbance of the debris-flow gully, the earthquake amplification effect should be considered in calculating the discharge and magnitude of debris flows during seismically active periods.

We proposed a systematic and quantitative hazard analysis method for the burring, impacting, and scouring hazards induced by debris flow. This method was applied to the case study of debris flows in Ridi Gully, and we predicted potential hazards and their influence on the Sichuan-Tibet railway (or highway) and the residential area on the alluvial fan. The results may play a significant role in disaster prevention and mitigation during the Sichuan-Tibet railway (or highway) construction and maintenance. However, in the alpine areas of western China, especially in the eastern Qinghai-Tibet Plateau area, large-scale debris flows caused by heavy rainfall or glacier-lake outbursts commonly lead to complex and devastating damage. This damage manifests in a variety of ways, including direct impact destruction, debris accumulation, subsequent damage induced by destruction of infrastructure, and chain-reaction disasters that occur because of river blockages. The presented method considers disaster formation conditions, hazard indexes, and hazard-affected objects in hazard assessment for a debris flow. However, the risks of multiple debris flows are complex and beyond the ability of existing hazard analysis methods based singularly or primarily on debris flow. Therefore, this issue needs additional study to further facilitate risk analysis and disaster mitigation of debris flows.

Conclusions

The topography, geology, loose solid material, and water resource conditions are very favorable for debris-flow formation in the Ridi Gully. The simulation results currently indicate that the debris-flow peak discharge rate from upstream to downstream gradually increases. If no mitigation measures are implemented, debris flow will cause great damage to human life and three extremely significant infrastructure projects, especially the Sichuan-Tibet railway (or highway) construction.

Erosion is an important element to consider when analyzing the dynamic process of debris flow. We applied a dynamic erosion model and simulation method

to analyze the hazard characteristics of the debris movement process in Ridi Gully. During the process of debris flow, the structure of debris materials changed. The particles started to move and form a debris flow in the origin area (a catchment area), and stopped in the deposition area under the effect of slowing terrain conditions. Accordingly, different dynamic characteristics, including strong erosion and debris impact hazards, scouring and downward erosion, and siltation, are displayed in the debris-flow origin area, transition area, and accumulation area of Ridi Gully, respectively.

Reasonable and quantitative assessment of the hazards associated with debris flows is complex. Accordingly, we established indicators to describe compound disasters induced by debris flow, and provided a quantitative method for analyzing the hazards associated with a debris flow in the Ridi Gully in the eastern Qinghai-Tibet Plateau area. The capacities for debris impact damage and silting damage were quantified using the maximum values of kinetic energy and flow depth, respectively. Finally, we predicted the hazard and its influence on the human environment. The Sichuan-Tibet railway (or highway) and the residential area on the alluvial fan suffer from large risks of debris flow, which is consistent with the actual situation determined from field observation. Thus, this successful validation strongly suggests that the high level of debris-flow hazard simulated by the proposed method may serve as pertinent and timely evidence to help prevent or reduce the debris-flow hazard in the eastern Qinghai-Tibet Plateau area and beyond.

Acknowledgments

This research was supported by the National Nature Science Foundation of China (Grant No. 41401598), the project of Science and Technology Service Network Plan of Chinese Academy of Sciences (Grant No.KFJ-EW-STS-094), the Technological Achievements Popularization Project of Chinese Transport Ministry (Grant No. 2015316T19060), and the Research Foundation of Key Laboratory of Digital Mapping and Land Information Application of National Administration of Surveying, Mapping and Geoinformation (Grant No. DM2016SC03), and the Youth Innovation Promotion Association of Chinese Academy of Sciences.

References Cited

Anderson, S. A., and Sitar, N., 1996: Analysis of rainfall-induced debris flows. *Journal of Geotechnical Engineering*, 122(7): 544–552.

Archetti, R., and Lamberti, A., 2003: Assessment of risk due to debris flow events. *Natural Hazards Review*, 4(3): 115–125.

Bisson, M., Favalli, M., Fornaciai, A., Mazzarinia, F., Isolaa I., Zanchettab, G., and Pareschia, M. T., 2005: A rapid method to assess fire-related debris flow hazard in the Mediterranean region: an example from Sicily (southern Italy). *International Journal of Applied Earth Observation and Geoinformation*, 7(3): 217–231.

Calvo, B., and Savi, F., 2009: A real-world application of Monte Carlo procedure for debris flow risk assessment. *Computers and Geosciences*, 35(5): 967–977.

Chen, N. S., 2011: *Debris Flow Exploration Technology*. Beijing: Science Press, 161–165. (in Chinese).

Chen, N. S., Cui, P., Liu, Z. G., and Wei, F. Q., 2003: Calculation of the debris flow concentration based on clay content. *Science in China (Series E), Technological Sciences*, 33(Supp.): 164–174.

Cui, P., Zhuang, J. Q., Chen, X. C., Zhang, J. Q., and Zhou, X. J., 2010: Characteristics and countermeasures of debris flow in Wenchuan area after the earthquake. *Journal of Sichuan University (Engineering Science Edition)*, 42(5): 10–19 (in Chinese).

Cui, P., Xiang, L. Z., and Zou, Q., 2013: Risk assessment of highways affected by debris flows in Wenchuan earthquake area. *Journal of Mountain Science*, 10(2): 173–189.

Dhital, M. R. 2015: *Geology of the Nepal Himalaya: Regional Perspective of the Classic Collided Orogen*. Berlin: Springer.

Fei, X. J., and Shu, A. P. (eds.), 2004: *Movement Mechanism and Disaster Control for Debris Flow*. Beijing: Tsinghua University Press, 114-119. (in Chinese).

Fuchs, S., Kaitna, R., Scheidl, C., and Hübl, J., 2008: The application of the risk concept to debris flow hazards. *Geomechanics and Tunnelling*, 1(2): 120–129.

Gentile, F., Bisantino, T., and Liuzzi, G. T., 2008: Debris-flow risk analysis in south Gargano watersheds (southern-Italy). *Natural Hazards*, 44(1): 1–17.

Grêt-Regamey, A., and Straub, D., 2006: Spatially explicit avalanche risk assessment linking Bayesian networks to a GIS. *Natural Hazards Earth System Science*, 6: 911–926.

Han, Z., Chen, G., Li, Y., Tang, C., Xu, L., He, Y., Huang, X., and Wang, W., 2015: Numerical simulation of debris-flow behavior incorporating a dynamic method for estimating the entrainment. *Engineering Geology,* 190: 52–64.

Hübl, J., Suda, J., Proske, D., Kaitna, R., and Scheidl, C., 2009: Debris flow impact estimation. *In Proceedings of the 11th International Symposium on Water Management and Hydraulic Engineering*, 137–148.

Huggel, C., Kaab, A., Haeberli, W., and Krummenacher, B., 2003: Regional-scale GIS-models for assessment of hazards from glacier lake outbursts: evaluation and application in the Swiss Alps. *Natural Hazards and Earth System Sciences,* 3: 647–662.

Hürlimann, M., Copons, R., and Altimir, J., 2006: Detailed debris flow hazard assessment in Andorra: a multidisciplinary approach. *Geomorphology*, 78(3): 359–372.

Iverson, R. M., 2012: Elementary theory of bed-sediment entrainment by debris flows and avalanches. *Journal of Geophysical Research Atmospheres*, 117(F3): 259–281.

Jakob, M., Hungr, O., and Jakob, D. M., 2005: Debris-flow hazards and related phenomena. Berlin: Springer.

Lin, C. W., Shieh, C. L., Yuan, B. D., Shieh, Y. C., Liu, S. H., and Lee, S.Y., 2004: Impact of Chi-Chi earthquake on the occurrence of landslides and debris flows: example from the Chenyulan River watershed, Nantou, Taiwan. *Engineering Geology*, 71(1): 49–61.

Liu, J., Nakatani, K., and Mizuyama, T., 2012: Effect assessment of debris flow mitigation works based on numerical simulation by using Kanako 2D. *Landslides*, 10(2): 161–173.

Mark, R. K., and Ellen, S. D., 1995: Statistical and simulation models for mapping debris-flow hazard. *In* Carrara, A., and Guzzetti, F. (eds.), *Geographical Information Systems in Assessing Natural Hazards*, vol. 5. Netherlands: Springer, 93–106.

Marzocchi, W., Garcia-Aristizabal, A., Gasparini, P., Mastellone, M. L., and Ruocco, A. D., 2012: Basic principles of multi-risk assessment: a case study in Italy. *Natural Hazards*, 62(2): 551–573.

Okunishi, K., and Suwa, H., 2001: Assessment of debris-flow hazards of alluvial fans. *Natural Hazards*, 23(2–3): 259–269.

Ouyang, C. J., He, S. M., and Tang, C., 2015: Numerical analysis of dynamics of debris flow over erodible beds in Wenchuan earthquake-induced area. *Engineering Geology*, 194: 62–72.

Pradhan, B., 2010: Remote sensing and GIS-based landslide hazard analysis and cross-validation using multivariate logistic regression model on three test areas in Malaysia. *Advances in Space Research*, 45: 1244–1256.

Rickenmann, D., 1999: Empirical relationships for debris-flows. *Natural Hazards*, 19(1): 47–77.

Shou, K. J., Wu, C. C., Fei, L.Y., Lee, J. F., and Wei, C.Y., 2011: Dynamic environment in the Ta-Chia River watershed after the 1999 Taiwan Chi-Chi earthquake. *Geomorphology*, 133(3): 190–198.

Sichuan Provincial Water Conservancy and Electric Power Department, 2010: *The Rainstorm and Flood Calculation Manual of Medium and Small Basins in Sichuan Province.* Chengdu: Sichuan Provincial Water Conservancy and Electric Power Department Press (in Chinese).

Sun, P., Zhang, Y. S., Shi, J. S., and Chen, L. W., 2011: Analysis on the dynamical process of Donghekou rockslide-debris flow triggered by 5.12 Wenchuan earthquake. *Journal of Mountain Science,* 8(2): 140–148.

Wu, J. S., Tian, L. Q., Kang, Z. C., Zhang, Y. F., and Liu, J., 1993: *Debris Flow and Its Comprehensive Control*. Beijing: Science Press, 44–48 (in Chinese).

Xiang, L. Z., Cui, P., Zhong, D. L., Ge, Y. G., Zhu, X. H., and Yang, W., 2012: Quantitative hazard assessment of road debris flow in Wenchuan earthquake area: a case study of Xiaojia Ravine in Wenchuan County. *Journal of Southwest Jiaotong University*, 47(3): 387–393 (in Chinese).

You, Y., Liu, J. F., and Chen, X. C. 2010: Debris flow and its characteristics of Subao River in Beichuan County after "5·12" Wenchuan earthquake. *Journal of Mountain Science*, 28(3): 358–366 (in Chinese).

Zhou, B. F., Li, D. J., and Luo, D. F., 1991: *Guide to Prevention of Debris Flow*. Beijing: Science Press (in Chinese).

Zou, Q., Cui, P., Zeng, C., Tang, J. X., and Regmi, A. D., 2016: Dynamic process-based risk assessment of debris flow on a local scale. *Physical Geography*, (37)2: 132–152.

MS submitted 7 February 2017
MS accepted 3 May 2017